

Constant contribution in meson correlators at finite temperature

Takashi Umeda

Physics Department, Brookhaven National Laboratory, Upton, NY 11973, USA

(Dated: November 1, 2018)

We discuss a constant contribution to meson correlators at finite temperature. In the deconfinement phase of QCD, a colored single quark state is allowed as a finite energy state, which yields to a contribution of wraparound quark propagation to temporal meson correlators. We investigate the effects in the free quark case and quenched QCD at finite temperature. The “scattering” contribution causes a constant mode in meson correlators with zero spatial momentum and degenerate quark masses, which can dominate the correlators in the region of large imaginary times. In the free spectral function, the contribution yields a term proportional to $\omega\delta(\omega)$. Therefore this contribution is related to transport phenomena in the quark gluon plasma. It is possible to distinguish the constant contribution from the other part using several analysis methods proposed in this paper. As a result of the analyses, we find that drastic changes in charmonium correlators for χ_c states just above the deconfinement transition are due to the constant contribution. The other differences in the χ_c states are small. It may indicate the survival of χ_c states after the deconfinement transition until, at least, $1.4T_c$.

PACS numbers: 12.38.Gc, 12.38.Mh

I. INTRODUCTION

In the imaginary time formalism of finite temperature field theory, temporal correlators are related to several dynamical properties through a prescription of analytical continuation. Especially the imaginary time correlator can be described by the same spectral function as that of retarded and advanced green functions. Therefore the spectral functions extracted from the imaginary time correlators, which are able to be calculated in lattice QCD, enable us to investigate important physics at finite temperature, e.g. dilepton rates [1], light mesons [2], heavy quarkonia [3, 4, 5, 6, 7, 8], glueballs [9], transport coefficients [10, 11, 12].

One of the most important quantities at finite temperature QCD is the spectral function of heavy quarkonium, which plays the key role for understanding the quark gluon plasma (QGP) formation in heavy ion collision experiments e.g. the RHIC experiment at Brookhaven National Laboratory. Recent studies on the spectral function of charmonium above T_c suggest that hadronic excitations corresponding to J/ψ may survive in the deconfinement phase till relatively high temperature [4, 5, 6, 7, 8]. Such results of strongly interacting QGP may affect the scenario of J/ψ suppression [13, 14]. Therefore the determination of the accurate dissociation temperature of J/ψ is required for many phenomenological studies.

As somewhat different from the “direct” J/ψ suppression, recently an “indirect” J/ψ suppression was proposed [15, 16]. The total yield of J/ψ is not only from the direct production, about 40% of the J/ψ 's that come from the higher states ψ' and χ_c [17]. If the higher states dissociate at lower temperatures, a part of the J/ψ suppression may be observed in experiments at a lower temperature than that of J/ψ . Therefore the study of ψ' and χ_c states and their dissociation temperatures is a very interesting subject for the physics of QGP. Several

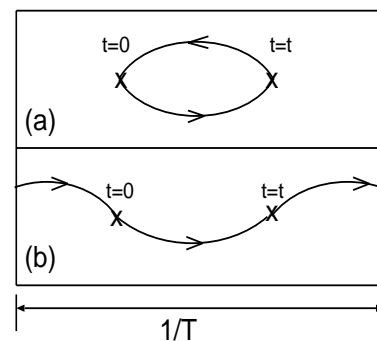


FIG. 1: A sketch of quark line diagrams for a meson-like correlator in a system with finite temporal extent. Vertical lines show the boundaries in temporal direction.

groups have already investigated the χ_c states, and their results indicate that the lowest peak of the spectral function, corresponding to the χ_c state, may dissociate just after the transition temperature [5, 7, 8]. On the other hand there is no lattice QCD study on the ψ' states above T_c , because it is difficult to extract information of non-lowest states such as ψ' from the correlator on the lattice at finite temperature.

In such studies of temporal correlators at finite temperature, one has to take account of a characteristic contribution caused by the finite temporal extent. Usually a meson correlator is interpreted by a diagram with quark and anti-quark propagators like it is sketched in Fig. 1(a). However in the case of a system with a finite temporal extent, a wraparound (scattering) contribution, as shown in Fig. 1(b), has to be included as well. It is similar to the situation at zero temperature e.g. the study of two pion correlators [18], and pentaquark correlator [19]. Because these correlators include multi-hadron states as intermediate states, and each state is also allowed as a

color singlet state, which can have a finite energy state in the confined phase. At zero temperature the calculation should be performed, in principle, with infinite temporal extent, therefore, the wraparound effect is not physical. The contribution is usually removed using e.g. Dirichlet boundary conditions [19] or appropriate analyses [18].

In finite temperature calculations using the imaginary time formalism, the temporal extent is determined by (the inverse of) the temperature, and the quark fields have to have anti-periodic boundary conditions. In the confinement phase, an expectation value of the diagram in Fig.1(b) vanishes because it is related to a single quark propagation, which is exponentially suppressed with its infinite energy due to the confinement. On the other hand, in the deconfinement phase, the contribution may yield a finite expectation value. This is similar to the discussion of the Polyakov loop expectation value. For example in the free quark system, when one adopt a meson-like operator with degenerate quark masses and zero spatial momentum, the correlator of the diagram in Fig.1(a) behaves like $\exp(-m_q t) \times \exp(-m_q t) = \exp(-2m_q t)$, where m_q is the quark mass (or the energy of a single quark state). (Here we note that equations are written with dimension-less variables throughout this paper, if there is no comment on the units.) On the other hand, the diagram in Fig.1(b) behaves like $\exp(-m_q t) \times \exp(-m_q(L_t - t)) = \exp(-m_q L_t)$, where L_t is the inverse of the temperature. The latter diagram provides a constant contribution to the correlator, and the contribution may dominate in the large imaginary time region as a zero energy mode. Due to the contribution, correlators of such meson-like operators, e.g. charmonia, may be drastically changed just after the deconfinement transition. The latter type diagram, in general, yields t -dependent contributions which depends on a difference between single quark energies for each quark propagator. Even in non-degenerate quark masses or non-zero spatial momentum cases, the diagram can yield the constant contribution when the energies are identical. However we do not discuss the case in this paper. The finite momentum case has been discussed in Ref. [20] at high temperature limit.

This paper is organized as follows. In Sect. II we discuss the correlators of meson-like operators and its spectral functions in a system of free quarks with finite temporal extent. Some numerical results are also presented. In this section we also discuss the physical interpretation of the constant contribution and some analysis methods to avoid this contribution. In Sect. III we show numerical simulations in quenched QCD on anisotropic lattices, and demonstrate effects of the constant contribution in the interacting case and the analyses to avoid the contribution. As a result of these analyses we show that the χ_c state yields a small change except for the constant mode in its spectral function after the deconfinement transition like the J/ψ state at least up to $T = 1.4T_c$. At last we discuss results on the constant contribution.

II. THE CONSTANT CONTRIBUTION IN THE FREE THEORY

A. Meson-like correlators in the free quark case

In order to investigate the constant contribution as mentioned in the Introduction, we first consider the free quark case of QCD, in which the constant contribution can be easily calculated. Here we define the meson-like correlators with quark bilinear operators, $O_\Gamma(\vec{x}, t) = \bar{q}(\vec{x}, t)\Gamma q(\vec{x}, t)$, in the free quark case this gives for the correlator,

$$C(t) = \sum_{\vec{x}} \langle O_\Gamma(\vec{x}, t) O_\Gamma^\dagger(\vec{0}, 0) \rangle, \quad (1)$$

where Γ are appropriate 4×4 matrices, i.e. γ_5 , γ_i , 1 , and $\gamma_i \gamma_5$ for pseudoscalar (Ps), vector (V), scalar (S), and axialvector (Av) channels respectively. In this section and later we always adopt the anti-periodic boundary condition for quark fields in temporal direction to suppose a finite temperature case, and periodic boundary conditions in spatial directions. In this paper we calculate correlators for degenerate quark masses, constructed from bilinear operators, with vanishing spatial momentum as the simplest case, which is aiming at studies of charmonium at finite temperature discussed in Sect. III. The spectral function of the correlator is defined by

$$C(t) = \int_0^\infty d\omega \rho_\Gamma(\omega) K(\omega, t),$$

$$K(\omega, t) = \frac{\cosh\left(\omega\left(\frac{L_t}{2} - t\right)\right)}{\sinh\left(\omega\frac{L_t}{2}\right)}, \quad (2)$$

and has been calculated in Ref. [20, 21] in the high temperature limit.

In the spectral representation, the constant contribution provides a term proportional to $\omega \delta(\omega)$, which corresponds to a constant mode in the meson-like correlators. This term is an odd function in frequency ω , which is one of the basic properties of bosonic spectral function. From the results in [20, 21] one can find several characteristic properties of the constant contribution. First there is no constant mode in the Ps channel, however the other correlators have the constant mode, which comes from the scattering contribution. The correlator in the S channel has also no constant mode at vanishing quark mass, where the chiral symmetry is restored. Secondly, in the V channel (and the Av channel in the chiral limit), there is no constant contribution coming from the zero relative momentum process. On the other hand, there is one in the Av and S channels (and it disappears in chiral limit)¹. These properties are very important especially in

¹ One can find this property from the Table I of Ref. [21]. No constant mode and zero relative momentum correspond to $d_H^{lat} = 0$ and $d = 0$ (if quark mass is finite) respectively.

a finite volume calculation. When the minimum nonzero momentum due to the finite volume is large, the contribution of the zero relative momentum processes dominates in the correlators. Furthermore, a two quark state with zero relative momentum is forbidden in the P-wave state. Therefore the relative contribution of the constant mode increases exponentially as the spatial volume decreases in the P-wave state at finite quark mass. As a result, we can expect a very different behavior of correlators between S-wave and P-wave states in the case of finite quark mass and finite (but relatively small) volume. Thirdly, correlators for each channel coincide at the midpoint $t = L_t/2$ as mentioned in Ref. [20]. These characteristic properties will be confirmed also by the numerical results presented in the next section (II B).

It is important to consider physical interpretations of this contribution. The term $\omega\delta(\omega)$ remains in the continuum form and infinite volume results [20, 21], while it disappears at zero temperature, i.e. infinite temporal extent. Therefore the contribution is caused by a kind of physical thermal effect. The origin of the effect could be considered as a scattering with the thermal bath (Landau dumping) which is related to some transport coefficients. From the Kubo formula, for example, a derivative of the spectral function in the V channel, $\rho_V(\omega)$ which is defined by Eq. (2) using $\Gamma = \gamma_i$, is related to the electrical conductivity σ [11],

$$\sigma = \frac{1}{6} \frac{\partial}{\partial \omega} \rho_V(\omega) \Big|_{\omega=0}. \quad (3)$$

Let us also note on the dilepton rate. The dilepton rate is extracted from the spectral functions in the vector channel of spatial ($\rho_V(\omega)$ with $\Gamma = \gamma_i$) and temporal (ρ_{V_0} with $\Gamma = \gamma_0$) components,

$$\rho^{dilepton}(\omega) = \rho_V(\omega) + \rho_{V_0}(\omega). \quad (4)$$

$\rho_{V_0}(\omega)$ is the charge susceptibility and it has only the $\omega\delta(\omega)$ term which is equivalent to that of $\rho_V(\omega)$ with the opposite sign. Therefore the constant contribution in the dilepton rate cancels at least for the free quark case.

B. Free quark calculations on a lattice

In this subsection we present numerical calculations of the meson-like correlators for free quarks on lattices. The calculations are performed on isotropic $N_s^3 \times N_t = 16^3 \times 32$ lattices, and the volume dependence is discussed using results for $96^3 \times 32$ lattice. The free quark is described by the Wilson quark action with a bare quark mass of $m_q = 0.2$. The boundary conditions are anti-periodic in temporal direction and periodic in spatial directions.

Figure 2 shows correlators (Eq. (1)) for each channel. One can clearly see a constant contribution in the S and Av channels. The qualitative difference between the (Ps,V) and (S,Av) channels and the coincidence of

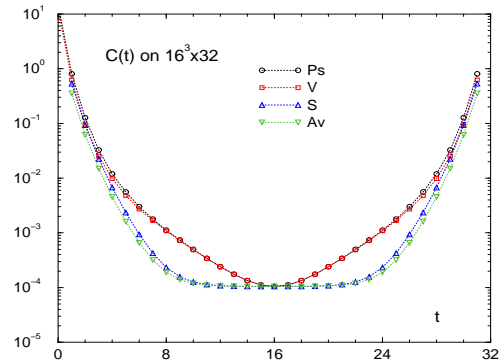


FIG. 2: Meson-like correlators for each channel. These are free quark calculations on a $16^3 \times 32$ lattice. The scale is logarithmic on the vertical axis.

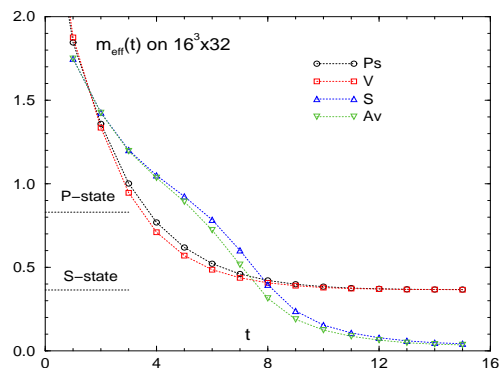


FIG. 3: Effective masses of meson-like correlators for each channel. These are free quark calculations on a $16^3 \times 32$ lattice.

correlators at the mid point $t = N_t/2$ can be explained as mentioned in the previous section.

Figure 3 shows the effective masses of the correlators in Fig. 2. The effective mass is defined by correlator at successive time slices.

$$\frac{C(t)}{C(t+1)} = \frac{\cosh [m_{\text{eff}}(t) (\frac{N_t}{2} - t)]}{\cosh [m_{\text{eff}}(t) (\frac{N_t}{2} - t - 1)]} \quad (5)$$

The effective masses of the meson-like correlators with free quarks should approach the energy of the two quark state without momentum for S-wave states (Ps and V channels) and with a minimum momentum for P-wave states (S and Av channels) except for the zero energy mode. In the Wilson quark action, the free quark propagator satisfies the dispersion relation,

$$\cosh E_q(p) = 1 + \frac{\sin^2(p_i) + (m_q + \hat{p}^2/2)^2}{2(1 + m_q + \hat{p}^2/2)}, \quad (6)$$

where $\hat{p}_i = 2 \sin(p_i/2)$ and $E_q(p)$ is the energy of a quark with momentum p_i . Using Eq. (6), one can calculate the lowest energies of the two quark states in S-wave and P-wave states. The values obtained for $N_s = 16$ and

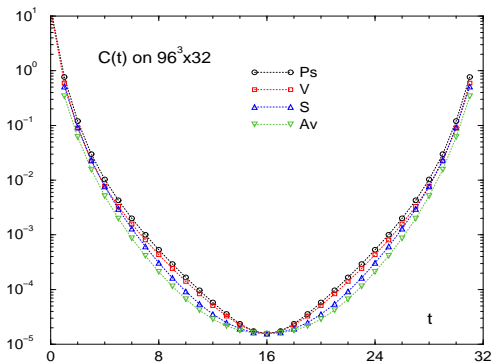


FIG. 4: Meson-like correlators for each channel. These are free quark calculations on a $96^3 \times 32$ lattice. The scale is logarithmic on the vertical axis.

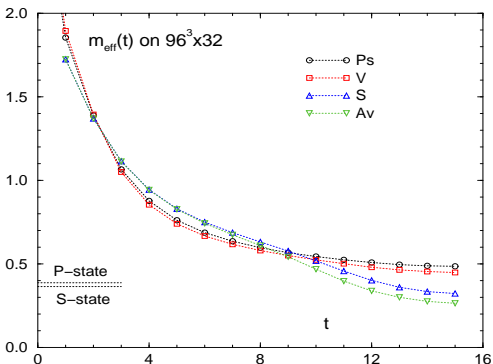


FIG. 5: Effective masses of meson-like correlators for each channel. These are free quark calculations on a $96^3 \times 32$ lattice.

$m_q = 0.2$ are shown in Fig. 3. In the Ps and V channels, the zero relative momentum processes have no constant contribution and their effective masses approach the expected values. In the S and Av channels, on the other hand, their effective masses approach the zero energy level rather than the energy of two quark states.

Next I present the results for the different volume. Figure 4 and 5 are results of the meson-like correlators and their effective masses on a $96^3 \times 32$ lattice with the same quark mass, $m_q = 0.2$, respectively. In the latter section (III), we present simulations in quenched QCD at finite temperature, where the finite temperature lattices have the similar aspect ratio, N_s/N_t , and the lowest state energy in lattice units to this free quark calculation with $N_s = 96$. Although we find the large volume dependence between $N_s = 16$ and $N_s = 96$, almost no volume dependence is seen for $N_s/N_t > 2$. At a sufficiently large aspect ratio, we find no clear constant contribution, but the finite constant contribution exists when the quark mass is finite.

C. An analysis to avoid the constant contribution and Polyakov loop sectors

Since the lattice QCD is formulated in Euclidean space-time, we can isolate the lowest state contribution from correlators in the large Euclidean time region, while studies of non-lowest states are not so easy. When one wants to know the information about nonzero energy states, the constant mode makes it difficult. The lowest scattering process yields only a constant mode in the correlators considered in this paper, and does not affect the other dynamics at higher energy, $\omega \geq 2m_q$, at least in the free quark case. Even in the case of interacting QCD, if the width of the peak structure in the spectral function at $\omega = 0$ is sufficiently small, e.g. $\omega \ll T$, the contribution yields only a constant mode in the correlators [10, 22]. Therefore, in order to investigate the nonzero energy states in the correlators, it is useful to remove the constant mode from the correlators in an appropriate analysis. In this subsection we present two analysis methods to avoid the constant contribution from the correlators.

Of course the cosh + constant fit enables us to do so, but here we present the methods without a fit analysis. The constant mode in the correlators can be removed by the derivative of the correlator with respect to t [23], where the differential correlator $C'(t)$ is defined by a derivative of $C(t)$,

$$C'(t) = C(t+1) - C(t). \quad (7)$$

Here $C'(t)$ is equivalent to the symmetric derivative at $t + 1/2$. One can define the effective mass of the differential correlator,

$$\frac{C'(t)}{C'(t+1)} = \frac{\sinh \left[m_{\text{eff}}^{\text{diff}}(t) \left(\frac{N_t}{2} - t \right) \right]}{\sinh \left[m_{\text{eff}}^{\text{diff}}(t) \left(\frac{N_t}{2} - t - 1 \right) \right]}. \quad (8)$$

Since, however, the overlap of each state is modified by a factor of the energy of the state in the analysis, the plateau of the effective masses becomes narrow. Furthermore, in general, a derivative of an observable increases the statistical fluctuations, thus the analysis may be difficult to apply to actual numerical calculations. Therefore we adopt a rather different approach to remove the constant contribution². We define the midpoint subtracted correlator,

$$\bar{C}(t) = C(t) - C(N_t/2). \quad (9)$$

One can also define the effective mass of the subtracted

² We thank Frithjof Karsch for the remark on the midpoint subtracted correlator.

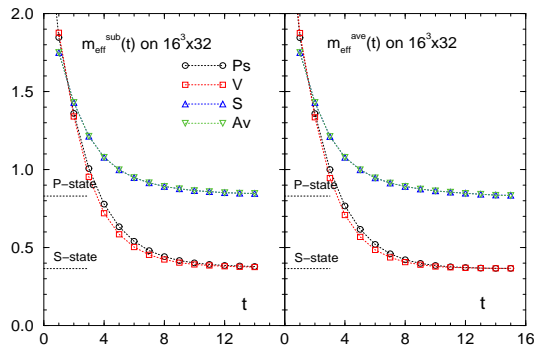


FIG. 6: Effective masses for each channel calculated from (left) the midpoint subtracted meson-like correlator and (right) the averaged correlator (averaged over the Polyakov loop sectors). These are free quark calculations on $16^3 \times 32$ lattices.

correlator,

$$\frac{\bar{C}(t)}{\bar{C}(t+1)} = \frac{\sinh^2 \left[\frac{1}{2} m_{\text{eff}}^{\text{sub}}(t) \left(\frac{N_t}{2} - t \right) \right]}{\sinh^2 \left[\frac{1}{2} m_{\text{eff}}^{\text{sub}}(t) \left(\frac{N_t}{2} - t - 1 \right) \right]}. \quad (10)$$

Figure 6 (left panel) shows the effective mass $m_{\text{eff}}^{\text{sub}}(t)$, defined in Eq. (10), from the free quark results for $N_s = 16$ in Fig. 2. The effective masses are equivalent to the usual effective mass shown in Fig. 3 except for the effects of the constant mode. The expected energies of the lowest two quark states for the S-wave and the P-wave states can be calculated from the free quark dispersion relation, Eq. (6). The values are shown in Fig. 6 as well as in Fig. 3. In contrast to the case of the usual effective masses in Fig. 3, the effective masses $m_{\text{eff}}^{\text{sub}}(t)$ approach the expected values even in the P-wave states. The analysis to avoid the constant contribution works well at least in the free quark case.

The method using the midpoint subtracted correlators can also be applied to studies of spectral functions $\rho_{\Gamma}(\omega)$ by a modification of the kernel,

$$\bar{C}(t) = \int_0^{\infty} d\omega \rho_{\Gamma}(\omega) K^{\text{sub}}(\omega, t), \quad (11)$$

$$K^{\text{sub}}(\omega, t) = \frac{2 \sinh^2 \left(\frac{\omega}{2} \left(\frac{N_t}{2} - t \right) \right)}{\sinh \left(\omega \frac{N_t}{2} \right)}. \quad (12)$$

By using the alternative kernel $K^{\text{sub}}(\omega, t)$, it is possible to extract the spectral function without the contribution in $\omega \ll T$ from e.g. the Maximum Entropy Method.

Next we consider the second method to avoid the constant contribution. The method utilizes the Z_3 transformation properties of the correlators, where the Z_3 transformation is performed on the lattice through the transformation of temporal link variables,

$$U_4(\vec{x}, t) \rightarrow e^{i2n\pi/3} U_4(\vec{x}, t), \quad (13)$$

where $n = 0, 1$ and 2 , for any \vec{x} , at a time slice (we adopt $t = N_t/2$). First we consider the Z_3 transformation properties for the diagrams in Fig. 1(a) and (b). The contribution of Fig. 1(a) has a Z_3 center symmetry, while that of Fig. 1(b) is no longer invariant under the Z_3 transformation. In case of the static limit, one can easily understand it by the analogy of Polyakov loop and Wilson loop. Even in the non-static case, the properties can be derived using a hopping parameter expansion of the quark propagator. In any order of the expansion, one can show this property like in the static limit.

Furthermore, for the Z_3 variant contribution, the Z_3 factor can be factored out. Therefore one can cancel the Z_3 variant contribution by averaging the correlators over the three sectors which are characterized by the location of the Polyakov loop in the complex plane. Here we define the averaged correlator $C^{\text{ave}}(t)$ from $C^{p0}(t)$, $C^{p1}(t)$ and $C^{p2}(t)$, which are correlators on the configurations with an argument of the Polyakov loop in the complex plane fulfilling $-\frac{2\pi}{3} \leq \arg(P) \leq \frac{2\pi}{3}$, $\frac{2\pi}{3} \leq \arg(P) \leq \pi$ and $-\pi \leq \arg(P) \leq -\frac{2\pi}{3}$ respectively, where P is a value of the Polyakov loop on the given configuration,

$$C^{\text{ave}}(t) = \frac{1}{3} (C^{p0}(t) + C^{p1}(t) + C^{p2}(t)). \quad (14)$$

Each correlator can be calculated on the Z_3 transformed gauge configurations.

The second method to avoid the constant contribution is in a way similar to removing the backward quark propagations by using a cancellation between results with periodic and anti-periodic boundary conditions in the t direction. However the second method is beyond a technical step to separate the constant mode from the others. The effect of Z_3 symmetrization is to remove from the partition function all states with non-integer baryon number (whether in quenched or full QCD). This has been discussed, e.g., in Ref. [24].

Here we should mention that the cancellation of the constant mode is not exact in the second method. Because, e.g., in the case of a diagram with a 3 times wrapping quark line, the contribution also has the Z_3 center symmetry. Therefore it will not be canceled in the analysis. (This situation is also similar to the cancellation of the backward quark propagation as mentioned above. This cancellation is also not exact. The remaining Z_3 symmetric contribution can be removed by considering the zero-baryon partition function, as discussed as well in Ref. [24].) However, the Z_3 invariant constant contributions is of $O(e^{-3m_q L_t})$ or less, while that for the leading (canceled) contribution is $O(e^{-m_q L_t})$. Therefore the averaged correlator is useful to see a qualitative effect of the constant contribution in the correlators, when $m_q L_t$ is not so small.

From the averaged correlator in Eq. (14), one can de-

fine the effective mass $m_{\text{eff}}^{\text{ave}}(t)$,

$$\frac{C^{\text{ave}}(t)}{C^{\text{ave}}(t+1)} = \frac{\cosh \left[m_{\text{eff}}^{\text{ave}}(t) \left(\frac{N_t}{2} - t \right) \right]}{\cosh \left[m_{\text{eff}}^{\text{ave}}(t) \left(\frac{N_t}{2} - t - 1 \right) \right]}. \quad (15)$$

The effective masses $m_{\text{eff}}^{\text{ave}}(t)$ for the free quark case are presented in the right panel of Fig. 6. Similar to the effective masses from the midpoint subtracted correlators, $m_{\text{eff}}^{\text{ave}}(t)$ approach the expected nonzero lowest energies even for the P-wave states. However the method does not exactly remove the constant contribution, a part of the constant contribution remains.

The method using the midpoint subtracted correlators does not work for correlators with finite momentum and non-degenerate masses of valence quarks, e.g. heavy-light meson. Although these cases are out of the scope of this study, the averaged correlator method works even for such meson-like operators. Furthermore provided the peak structure of spectral function at $\omega = 0$ has a wide width $\omega > T$ due to interactions, the subtracted correlator method may not even work in the case of correlators with zero momentum and degenerate quarks, while the averaged correlator method can be applied even in this case.

III. THE CONSTANT CONTRIBUTION IN QUENCHED LATTICE QCD AT FINITE TEMPERATURE

A. Lattice setup

In this section we demonstrate effect of the constant contribution and several analyses to avoid it in quenched QCD at finite temperature. In the simulation we calculate the charmonium correlators, which are defined like in Sect. II A at the charm quark mass. The temporal correlators (or the spectral functions) of charmonia are important to discuss the J/ψ suppression which is considered as one of the most important signals of QGP formation in heavy ion collision experiments. Several groups have investigated the charmonium correlators in finite temperature lattice QCD [4, 5, 6, 7, 8]. In such studies one has to take into account the constant contribution to the charmonium correlators (or spectral functions). Because this contribution may not be negligible in finite temperature lattice QCD. In fact it is a genuine effect in finite temperature QCD as mentioned in Sect. II A.

In finite temperature lattice QCD the temporal correlators are restricted within the inverse of the temperature. In order to keep sufficient number of data points in temporal direction at high temperature, we adopt an anisotropic lattice, on which the temporal lattice spacing a_t is smaller than the spatial one a_s . The temperature is varied by the temporal lattice sizes N_t with a fixed temporal lattice spacing a_t . Such calculations with a

fixed lattice spacing also have the advantage to investigate thermal effects in correlators, i.e. one can directly compare the correlators at different temperatures without need for information on the beta-function. In this section physical quantities are expressed in $a_t = 1$ units when there is no comment on the units.

The gauge configurations have been generated by an standard plaquette gauge action with a lattice gauge coupling constant, $\beta = 6.10$ and a bare anisotropy parameter $\gamma_G = 3.2108$. The definition of the action and parameters are the same as that adopted in Ref. [25]. Lattice sizes are $20^3 \times N_t$ where $N_t = 160$ at $T = 0$ and $N_t = 32, 26$ and 20 at $T > 0$. The lattice spacings are $1/a_s = 2.030(13)$ GeV and $1/a_t = 8.12(5)$ GeV which are determined from the hadronic radius $r_0 = 0.5$ fm. The physical volume size is about $(2\text{fm})^3$ and temperatures at $N_t = 32, 26$ and 20 are $T = 0.88T_c, 1.08T_c$ and $1.40T_c$ respectively. The temperatures have been determined by the peak position of the Polyakov loop susceptibility from which we found the critical temperature around $N_t = 28$. The finite temperature lattices have been generated up to 300 configurations after 20,000 sweeps for equilibration, each configuration is separated by 500 sweeps to reduce the autocorrelation. At zero temperature, we have 60 configurations with the same condition. In the calculations, the error analysis is performed by the jackknife estimation.

For the quark fields, we adopt an $O(a)$ improved Wilson quark action with tadpole improved tree level clover coefficients. Although the definition of the quark action is the same as in Ref. [25], we adopt a different choice of the Wilson parameter $r = 1$ to suppress effects of lattice artifacts in higher states of charmonium [21]. Then the parameters in the quark action³ are $\kappa = 0.10109$, $c_E = 1.911$, $c_B = 3.164$ and $\gamma_F = 4.94$. Figure 7 shows the usual effective masses calculated with the parameters listed above. The results at zero temperature satisfy a relativistic meson dispersion relation with the same anisotropy as the renormalized gauge anisotropy $a_s/a_t = 4$. The left and right panels in Fig. 7 show the results from the local and spatial extended operators. The latter operators are defined by $O_\Gamma(\vec{x}, t) = \sum_{\vec{y}} \phi(\vec{y}) \bar{q}(\vec{x} - \vec{y}, t) \Gamma q(\vec{x}, t)$ with a smearing function $\phi(\vec{x})$ in Coulomb gauge. In this calculation the spatially extended operators are adopted only in the source operators, the sink operators are local in any cases. The smearing function is the same as that in Ref. [4], i.e. $\phi(\vec{x}) = \exp(-A|\vec{x}|^P)$ where A and P are parameters determined by a matching with the charmonium wave function as $A = 0.2275$ and $P = 1.258$.

From the zero temperature calculation with the spatially extended operators we obtain the charmonium masses in physical units, $m_{\eta_c} = 3033(19)$ MeV and

³ Our lattice setup is very similar to one of Ref. [8]. Although our notation of the parameters are different from theirs, the corresponding parameters are consistent with the ones they adopted.

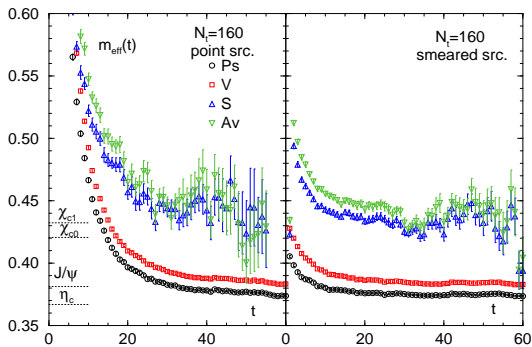


FIG. 7: Effective masses from charmonium correlators in quenched QCD at zero temperature. The left panel is the result with the local charmonium operators and the right one is the result with the spatially extended charmonium operators. Dotted lines in the left panel show the experimental values for each channel.

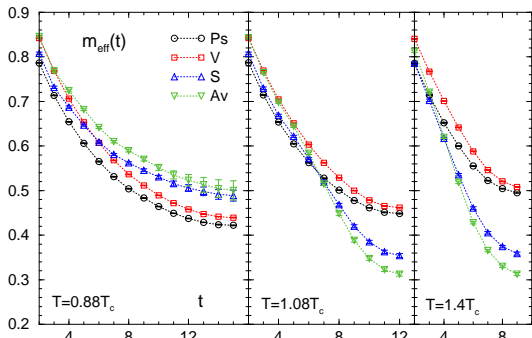


FIG. 8: Effective masses from charmonium correlators in quenched QCD at finite temperature. These are results with local operators for each channel.

$m_{J/\psi} = 3107(19)$ MeV, which are slightly heavier than their experimental values $m_{\eta_c}^{\text{exp.}} = 2980$ MeV and $m_{J/\psi}^{\text{exp.}} = 3097$ MeV [26]. The experimental values in lattice units are also shown in Fig. 7. The results for the P-wave states are rather noisy at our current statistics, and the actual values are not so important for this study. Therefore we do not show the numbers in MeV, however their effective masses show a plateau at reasonable values.

B. Finite temperature results

In this section we discuss the result of the charmonium correlators at finite temperature. The definitions for several types of effective masses can be taken over from that of the free quark calculations in Sect. II. First we show the usual effective masses, $m_{\text{eff}}(t)$ at finite temperature in Fig. 8. Since these are results obtained with local operators, there is no plateau region at any temperature or channel we chose. It can be expected from zero temperature calculation and the effective masses show reasonable

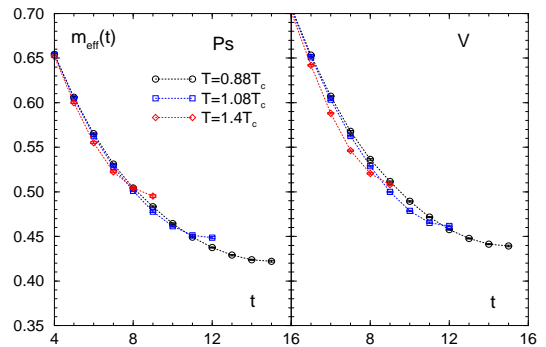


FIG. 9: Temperature dependence of the effective masses from charmonium correlators in quenched QCD at finite temperature. The left panel shows the Pseudoscalar (Ps) channel and the right one is the Vector (V) channel. These lowest states correspond to η_c and J/ψ .

behavior below T_c , at which the charmonium correlators does not show large difference from the zero temperature results [4, 5, 8]. We find rather large statistical fluctuations in the P-wave states, a reason for that is given later. Just above T_c , we see drastic changes in the P-wave state channels. The changes may cause the dissolution of χ_c states just above T_c as already reported in Ref. [5, 7, 8].

On the other hand, the S-wave states, i.e. the Ps and V channels, show small changes up to $1.4T_c$. This temperature dependences are shown in Fig. 9 for each channel. When we compare the effective masses at the same time slices, we find no large change up to $1.4T_c$ in both channels as well. The results are consistent with previous lattice studies of charmonium spectral functions [4, 5, 6, 7, 8], in which the spectral functions for the Ps and V channels in the deconfinement phase (but at not so high temperature) show a peak structure around the η_c and J/ψ masses like the result at zero temperature.

C. Midpoint subtracted correlator analysis

As discussed for free quarks in Sect. II, the constant contribution may dominate the meson correlators for some channels in the deconfinement phase. In order to see the contribution in the meson correlators we calculate the effective mass from the midpoint subtracted correlator, $m_{\text{eff}}^{\text{sub}}(t)$ defined in Eq. (10). Figure 10 shows the results of $m_{\text{eff}}^{\text{sub}}(t)$ in quenched QCD at finite temperature. As we expected, the effective masses at each temperature in the S-wave states show small differences from that of zero temperature, when comparing them at the same time slices. In the P-wave states, however, the drastic changes of the usual effective masses $m_{\text{eff}}(t)$ are absent in the effective masses from the midpoint subtracted correlators $m_{\text{eff}}^{\text{sub}}(t)$. Furthermore the similar behaviors of the effective masses hold till $1.4T_c$ as in the case of the S-

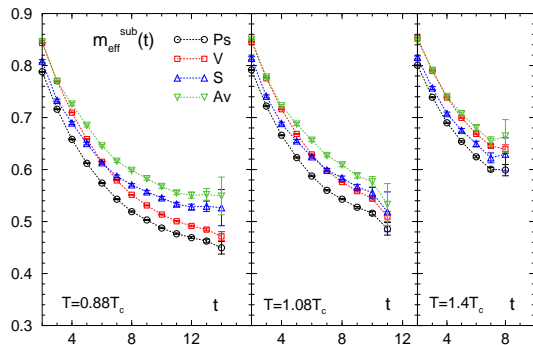


FIG. 10: Effective masses from the midpoint subtracted charmonium correlators in quenched QCD at finite temperature. These are results with local operators for each channel.

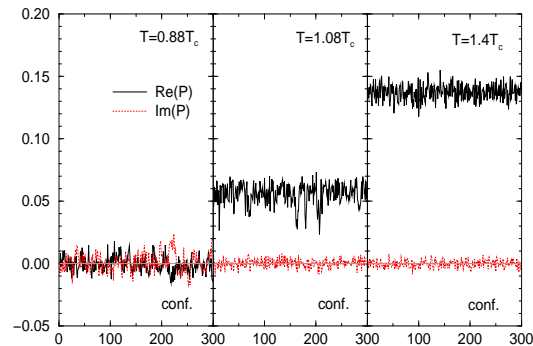


FIG. 11: Time histories of the real and imaginary part of the Polyakov loop P at each temperature simulation.

wave states. The results indicate that the drastic changes of the usual correlators (and effective masses) are caused only by the constant contribution to the correlators. The situation is very similar to the free quark case discussed in Sect. II.

D. Polyakov loop sector dependence of correlators

Next we discuss the Polyakov loop sector dependence of meson correlators as mentioned in Sect. II C. First of all we show time histories of the Polyakov loop on our finite temperature configurations in Fig. 11. For all configurations above T_c the Polyakov loop lies in the real sector.

Thus Fig. 8 gives the result on configurations with the Polyakov loop being in the real sector. The correlators for the imaginary sectors are calculated on configurations generated by Z_3 transformations from that in the real sector. As an example for the imaginary sectors we show the effective masses calculated from $C^{p0}(t)$, $C^{p1}(t)$, $C^{p2}(t)$ and $C^{\text{ave}}(t)$, which are defined in Sect. II C, in Fig. 12. As discussed in Sect. II C, the Z_3 transformation changes a part of the constant contribution by a factor of Z_3 , i.e. $e^{i2n\pi/3}$ where $n = 0, 1$ and 2 . Since our definition of the meson correlators is real, the factor acts like

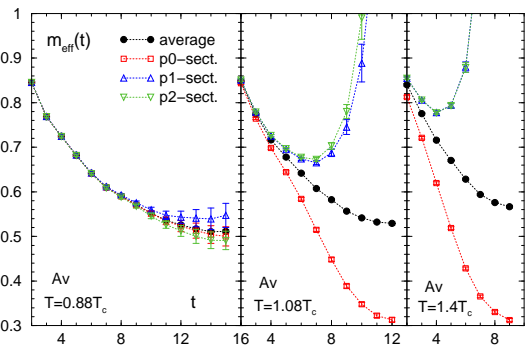


FIG. 12: Polyakov loop sector dependence of Effective masses for the Av channel. p0, p1 and p2 sector means the result has been obtained on configurations with the Polyakov loop restricted to the real and (positive and negative) imaginary sectors respectively. Average means averaged over all sectors as in Eq. (14).

$\text{Re}(e^{i2n\pi/3})$. It means that the constant contributions in the imaginary sectors become negative when the value in the real sector is positive. Hence the correlators of the P-wave states approach a positive constant value like in the real sector, as shown in Fig. 2, while the correlators for the imaginary sectors approach a negative value. As a result the effective masses of the P-wave states diverge at a time slice as shown in Fig. 12.

Here we comment on the large statistical fluctuations of correlators for the P-wave states just below T_c as can be seen in Fig. 8. Below T_c , in principle, the constant contribution vanishes due to the infinite energy of a single quark state in the confinement phase. However the contribution on each configuration may have a small value near T_c even in confinement phase, like the Polyakov loop just below T_c in Fig. 11. In this case the effect of the constant contribution appears in the correlators. Since the Polyakov loop sector frequently changes below T_c , the effects appear as the large fluctuation in the correlators.

When the averaged correlator defined in Eq. (14) is calculated, one can expect that most of the constant contributions are canceled like in the free quark case (Sect. II C). Figure 13 shows the results of $m_{\text{eff}}^{\text{ave}}(t)$ at each temperature. We find almost the same behavior as in Fig. 10. The results also suggest that the drastic changes in the P-wave states just above T_c are coming from the constant contribution only.

E. Results with spatially extended operators

Finally we present results of meson correlators with spatially extended operators. The spatially extended operators are constructed with a smearing function which yields a spatial distribution of quark (and anti-quark) source(s). The distribution also changes the momentum distribution of the quark propagation. For example, a point source function yields any (lattice) momenta with

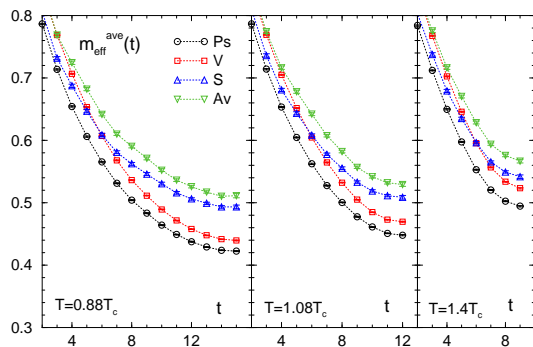


FIG. 13: Effective masses from the averaged charmonium correlators (averaged over the three sectors of the Polyakov loop) in quenched QCD at finite temperature. Configurations with the Polyakov loop in the imaginary sectors have been obtained by a Z_3 transformation of the corresponding real sector configuration. These are results with local operators for each channel.

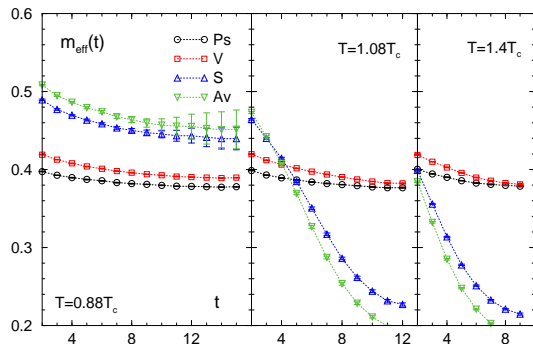


FIG. 14: The same as in Fig. 8 but for spatially extended operators in each channel.

equal distribution, while a wall source function yields only quark propagation with zero momentum. In the case of our source the (smearing) function provides quark propagation with any momenta but quark propagators with small momentum are enhanced. Therefore the correlators with spatially extended operators defined, as in Sect. III A, yield (relatively) large overlap with the lower energy states.

Figure 14 is the result for the usual effective masses with the spatially extended operators. Other conditions are the same as in Fig. 8. Below T_c , in contrast to the case of local operators the effective masses reach a plateau due to the larger overlap with the lowest state. Above T_c the effective masses of the P-wave states change more than in the case of local operators. Because the constant contribution is enhanced by the smearing function more than the other contributions in the case. The effect of the constant contribution is also present in the V channel. At least in the free quark case, as we discussed in Sect. II A, the constant contribution to the V channel is smaller than that to the P-wave states for finite quark masses and small volumes. In fact, even in quenched QCD, it is difficult to see the effect in the V channel in

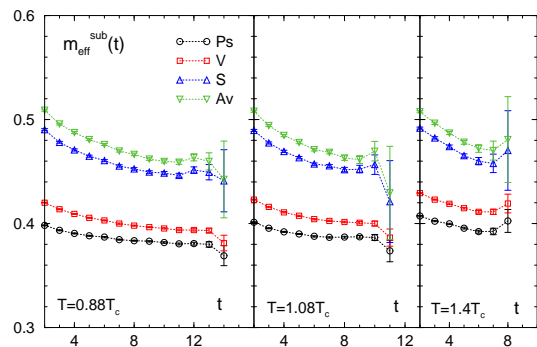


FIG. 15: The same as in Fig. 10 but for spatially extended operators in each channel.

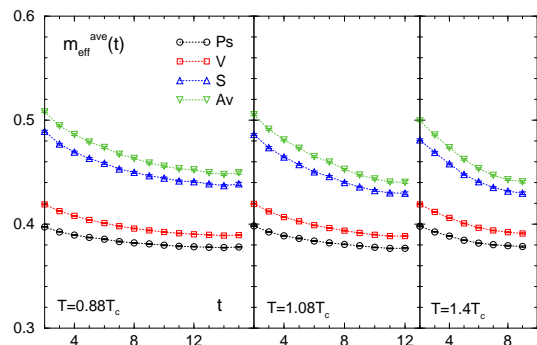


FIG. 16: The same as in Fig. 13 but for spatially extended operators in each channel.

local operators. However we find small but finite changes even in the V channel above T_c while no changes are seen in the Ps channel as we expected.

We can say that the small changes in the V channel is caused by the constant contribution, because the analysis with the midpoint subtracted correlators shows almost no changes in the V channel above T_c as it can be seen in Fig. 15. Similar to the results with local operators, the effective masses of the P-wave states also show small change at any temperatures.

Figure 16 is the same figure as Fig. 13, but with spatially extended operators. We find similar behavior for both cases of operators.

IV. DISCUSSION

Let us discuss details on χ_c states using the results of the previous sections. In this study we find that the drastic changes of the (usual) correlators in the P-wave states are caused by the constant contribution, while the correlators without the constant mode yield small change till, at least, $1.4T_c$ even in the P-wave states. The changes are of similar size as that of the S-wave states as one can see in Fig. 17 and Fig. 18.

In the case of the spatially extended operators, the averaged effective mass $m_{\text{eff}}^{\text{ave}}(t)$ for the Av channel grad-

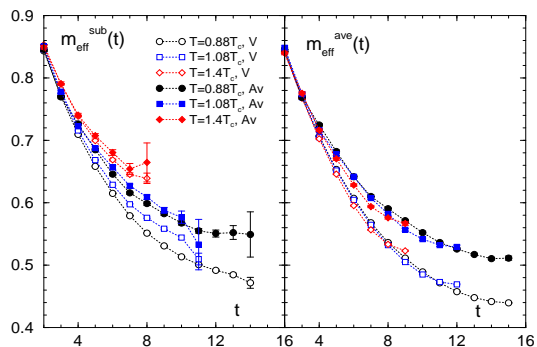


FIG. 17: Temperature dependences of the effective masses from the midpoint subtracted charmonium correlators (left) and the averaged charmonium correlators (averaged over the three sectors of the Polyakov loop) (right) in quenched QCD at finite temperature. These are results with local operators of the V and the Av channels, whose lowest states correspond to the J/ψ and χ_{c1} states.

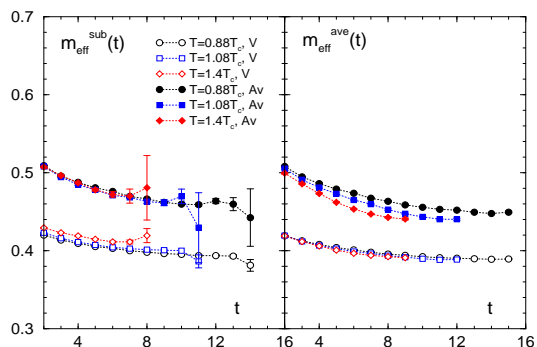


FIG. 18: The same as in Fig. 17 but for spatially extended operators in the V and the Av channels.

ually reduces as the temperature increases. The change seems to be effected by the constant contributions with the Z_3 center symmetry as discussed in Sect. II C. In fact, we can not find any hints of such a change in $m_{\text{eff}}^{\text{sub}}(t)$ in the left panel of Fig. 18. Furthermore it is reasonable to find the effect only in case of the spatially extended operators, because the Z_3 symmetric constant contribution is enhanced by the smearing function.

Although the constant mode coming from the scattering process is important to investigate some transport phenomena, it does not affect the spectral function in the $\omega \gg T$ region for the charmonium correlators with zero spatial momentum. Therefore the dissolution of χ_c states just above T_c as discussed in e.g. Ref. [5, 7, 8] might be misleading. When there is the constant contribution, the hadronic state is no longer the lowest state. The situation provides some difficulties in the analysis to reconstruct the spectral function in the higher energy part $\omega \gg T$ even if the MEM is applied [27]. The difficulties may be understood by the fact that most studies of the charmonium spectral function can not reproduce the excited states correctly especially at finite temperature

(even below T_c). Furthermore, in general, correlators for the P-wave states are noisier than that for the S-wave states as one can see in Fig. 7.

In principle the MEM analysis can extract the correct spectral function even if the constant contribution exists, however it is difficult to reproduce the non-lowest part of the spectral function correctly by the MEM analysis at finite temperature with typical statistics. In order to investigate the properties of χ_c states above T_c , a careful analysis taking the constant contribution into account is necessary. A correct MEM analysis of the correlator with and without the constant contribution should give the same results, up to the low energy region $\omega \ll T$. Such a comparison can be easily performed by the MEM analysis with the alternative kernel of Eq. (12) for midpoint subtracted correlators. Failure to do so signals unreliable MEM results.

We also find a Polyakov loop sector dependence of the constant contribution in quenched QCD. To study transport coefficients from the behavior of spectral function at $\omega = 0$ one has to pay attention to the Polyakov loop sector especially in quenched QCD calculations. From a practical viewpoint, the dependence on the Polyakov loop sector is useful to estimate the constant contribution as discussed in Sect. II C and Sect. III D.

The constant contribution may also explain some other results of previous studies of temporal correlators. First, in the study of the spectral function at finite temperature by the MEM analysis, one sometimes find a kind of divergence of the spectral function near $\omega = 0$, it may be caused by the constant contribution. Of course it may be a simple failure of the analysis, however the contribution near $\omega = 0$ ought to exist except for the Ps channel. Secondly, in the S-wave states of charmonium, several groups have reported that the correlator for the Ps channel shows almost no change above the deconfinement transition, while that of the V channel shows a small but significant change [4, 8, 28]. This can also be seen from our calculation in Sect. III. It can be explained by the constant contribution as we did in this paper. Thirdly, when one considers a spatial boundary dependence of the charmonium spectrum at finite temperature as in Ref. [28], the P-wave states (in the free quark case) have the lowest energy using a “hybrid boundary”, which is an anti-periodic boundary in one spatial direction and periodic in the other directions. On the other hand, the P-wave state has a larger energy with periodic boundaries in any spatial directions. However the (usual) effective mass of the P-wave state correlators for free quark calculations provides a smaller value in periodic boundary conditions than in the hybrid boundary case. This unexpected behavior of the effective mass is also explained by the scattering processes because of suppression of the scattering contribution by the anti-periodic boundary in a spatial direction. Finally, the Polyakov loop sector dependence of the chiral order parameter in quenched QCD [29] may be also explained by the effect of (Z_3 variant) wrapped contributions in the chiral condensate.

As we discussed in the last section, the constant contribution affects the temporal correlators at finite temperature in various cases. Therefore it is important to take this contribution into account for studies of temporal correlators in lattice QCD at finite temperature.

Acknowledgments

The author thanks F. Karsch, S. Sasaki, S. Datta, T. Yamazaki, T. Doi, H. Matusufuru, P. Petreczky,

S. Aoki and C. Schmidt for helpful discussions and comments. This work has been authored under contract number DE-AC02-98CH1-886 with the U.S. Department of Energy. The simulations have been performed on supercomputers (NEC SX-5) at the Research Center for Nuclear Physics (RCNP) at Osaka University and (NEC SX-8) at the Yukawa Institute for Theoretical Physics (YITP) at Kyoto University.

-
- [1] F. Karsch, E. Laermann, P. Petreczky, S. Stickan and I. Wetzorke, *Phys. Lett. B* **530**, 147 (2002) [arXiv:hep-lat/0110208].
 - [2] P. de Forcrand *et al.* [QCD-TARO Collaboration], *Phys. Rev. D* **63**, 054501 (2001) [arXiv:hep-lat/0008005].
 - [3] T. Umeda, R. Katayama, O. Miyamura and H. Matusufuru, *Int. J. Mod. Phys. A* **16**, 2215 (2001) [arXiv:hep-lat/0011085].
 - [4] T. Umeda, K. Nomura and H. Matusufuru, *Eur. Phys. J. C* **39S1**, 9 (2005) [arXiv:hep-lat/0211003].
 - [5] S. Datta, F. Karsch, P. Petreczky and I. Wetzorke, *Phys. Rev. D* **69**, 094507 (2004) [arXiv:hep-lat/0312037].
 - [6] M. Asakawa and T. Hatsuda, *Phys. Rev. Lett.* **92**, 012001 (2004) [arXiv:hep-lat/0308034].
 - [7] G. Aarts, C. R. Allton, R. Morrin, A. P. O. Cais, M. B. Oktay, M. J. Peardon and J. I. Skullerud, *PoS LAT2006*, 126 (2006) [arXiv:hep-lat/0610065].
 - [8] A. Jakovac, P. Petreczky, K. Petrov and A. Velytsky, arXiv:hep-lat/0611017.
 - [9] N. Ishii, H. Suganuma and H. Matusufuru, *Phys. Rev. D* **66**, 094506 (2002) [arXiv:hep-lat/0206020].
 - [10] G. Aarts and J. M. Martinez Resco, *JHEP* **0204**, 053 (2002) [arXiv:hep-ph/0203177].
 - [11] S. Gupta, *Phys. Lett. B* **597**, 57 (2004) [arXiv:hep-lat/0301006].
 - [12] A. Nakamura and S. Sakai, *Phys. Rev. Lett.* **94**, 072305 (2005) [arXiv:hep-lat/0406009].
 - [13] T. Hashimoto, K. Hirose, T. Kanki and O. Miyamura, *Phys. Rev. Lett.* **57**, 2123 (1986).
 - [14] T. Matsui and H. Satz, *Phys. Lett. B* **178**, 416 (1986).
 - [15] F. Karsch, D. Kharzeev and H. Satz, *Phys. Lett. B* **637**, 75 (2006) [arXiv:hep-ph/0512239].
 - [16] S. Digal, P. Petreczky and H. Satz, arXiv:hep-ph/0110406.
 - [17] L. Antoniazzi *et al.* [E705 Collaboration], *Phys. Rev. Lett.* **70**, 383 (1993).
 - [18] C. Kim, *Nucl. Phys. Proc. Suppl.* **129**, 197 (2004) [arXiv:hep-lat/0311003].
 - [19] T. T. Takahashi, T. Umeda, T. Onogi and T. Kunihiro, *Phys. Rev. D* **71**, 114509 (2005) [arXiv:hep-lat/0503019].
 - [20] G. Aarts and J. M. Martinez Resco, *Nucl. Phys. B* **726**, 93 (2005) [arXiv:hep-lat/0507004].
 - [21] F. Karsch, E. Laermann, P. Petreczky and S. Stickan, *Phys. Rev. D* **68**, 014504 (2003) [arXiv:hep-lat/0303017].
 - [22] P. Petreczky and D. Teaney, *Phys. Rev. D* **73**, 014508 (2006) [arXiv:hep-ph/0507318].
 - [23] P. Majumdar, Y. Koma and M. Koma, *Nucl. Phys. B* **677**, 273 (2004) [arXiv:hep-lat/0309003].
 - [24] S. Kratochvila and P. de Forcrand, *Phys. Rev. D* **73**, 114512 (2006) [arXiv:hep-lat/0602005].
 - [25] H. Matusufuru, T. Onogi and T. Umeda, *Phys. Rev. D* **64**, 114503 (2001) [arXiv:hep-lat/0107001].
 - [26] W. M. Yao *et al.* [Particle Data Group], *J. Phys. G* **33** (2006) 1.
 - [27] T. Umeda and H. Matusufuru, *PoS LAT2005*, 154 (2006) [arXiv:hep-lat/0510026].
 - [28] H. Iida, T. Doi, N. Ishii, H. Suganuma and K. Tsumura, *Phys. Rev. D* **74**, 074502 (2006) [arXiv:hep-lat/0602008].
 - [29] S. Chandrasekharan, D. Chen, N. H. Christ, W. J. Lee, R. Mawhinney and P. M. Vranas, *Phys. Rev. Lett.* **82**, 2463 (1999) [arXiv:hep-lat/9807018].